The self-consistent electronic structure of the interstitial compounds Fe_2B and FeB

1989 J. Phys.: Condens. Matter 1 1799

(http://iopscience.iop.org/0953-8984/1/10/002)

J. Phys.: Condens. Matter **1** (1989) 1799–1808. Printed in the UK

The self-consistent electronic structure of the interstitial compounds Fe_2B and FeB

Guangwei Li† and Dingsheng Wang†‡

† Institute of Physics, Academia Sinica, Beijing, People's Republic of China

‡ Center of Theoretical Physics, CCAST (World Laboratory), Beijing, People's Republic of China

Received 28 June 1988

Abstract. The linearised augmented plane-wave method and the local density functional potential are used to calculate the energy band and the density of states of two interstitial compounds Fe_2B and FeB and to give the distribution of the electron density showing the bonds between Fe and B and between B and B atoms. The calculated density of states agrees with photo-electron spectroscopy results. The B 2s and 2p states are well below the Fermi energy in both Fe_2B and FeB. Besides the metal bonds between Fe atoms, there exist strong covalent Fe–B bonds in Fe_2B. With the increase in B content, rather strong covalent B–B bonds form in FeB, leading to a one-dimensional zigzag chain structure. No electron transfer occurs between Fe and B atoms in these two compounds.

1. Introduction

Interstitial compounds consisting of relatively large transition-metal atoms and smaller metalloids have many useful properties, such as hardness, high melting point, wear resistance, corrosion resistance, good electric and thermal conduction, catalytic properties and ferromagnetism. These properties are characterised usually by covalent, ionic or metallic bonds. However, combination of these essentially different bonds may occur for interstitial compounds and thus lead to the development of materials with outstanding properties. The study of the electronic structure including the energy band, density of states and the electron distribution are consequently important for a thorough understanding of the properties of these interstitial compounds.

Both Fe_2B and FeB are typical interstitial compounds with ideal stoichiometry. Their electronic structures have been studied both experimentally (Brown and Cox 1971, Perkins and Brown 1974, Joyner *et al* 1980a,b, Joyner and Willis 1981) and theoretically (Johnson *et al* 1980, Joyner *et al* 1981). From x-ray diffraction and neutron scattering measurements of the charge and spin-density distribution, Brown and Cox (1971) and Perkins and Brown (1974) have suggested that the B 2s and 2p states in both Fe_2B and FeB are near the Fermi energy, and the difference between the two compounds is that, in Fe_2B, B 2s and 2p states, are completely unoccupied and, in FeB, only parts of them are occupied. The interaction between Fe and B atoms is so strong as to affect greatly the properties of the compounds notwithstanding whether the B 2s and 2p states are occupied or not. Joyner and Willis (1981) think that the distribution of the density of the valence states should be readily observable by photo-electron spectroscopy. The results

0953-8984/89/101799 + 10 $02.50

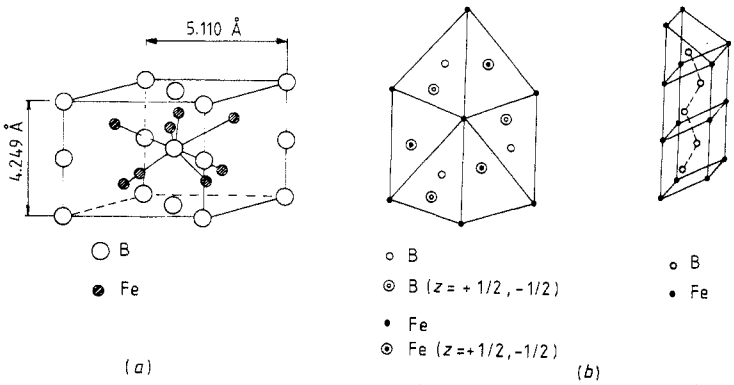

Figure 1. Crystal structure of (*a*) Fe_2B and (*b*) FeB projecting onto the (010) plane and for a section perpendicular to the plane (010) showing the zigzag B–B chain.

of the experiments, however, reveal that the B 2s and 2p states are well below the Fermi energy in both Fe_2B and FeB, which is significantly different from the previous model. It is inferred that B 2s and 2p states hybridise into the B 2sp state and form covalent bonds between B atoms in the two compounds. Up to now, no energy band calculation has yet been published for the two interstitial compounds. A detailed description of the bonds based on the distribution of electron density is missing.

In this paper, we give the electronic structures of Fe_2B and FeB from a first-principles calculation. Applying the linearised augmented plane-wave (LAPW) method (Koelling and Arbman 1975, Andersen 1975) and the local density functional potential (Hedin and Lundquist 1971), we self-consistently calculate the energy band and the density of states of both Fe_2B and FeB, give the distribution of the valence electron showing the bonds between Fe and B atoms and between B and B atoms and discuss the relations between the charge distribution and some properties of the two compounds, such as bonding characteristics, cohesion property, electron transfer and isomer shift.

2. Crystal structure and band method

2.1. Crystal structure

Fe_2B belongs to the body-centred tetragonal lattice ($a = b = 9.66$ au; $c = 8.032$ au) and the space group I4/mcm (Wever and Muller 1930). The B atoms in Fe_2B are between two layers of Fe atoms in a distorted closely packed arrangement, as shown in figure 1(*a*). A unit cell contains four equivalent Fe atoms in the positions of point group mm (type C16 with $x = 0.167$), and two equivalent B atoms in the positions of point group 42.

FeB belongs to the orthorhombic lattice ($a = 10.408$ au, $b = 5.580$ au and $c = 7.677$ au) and the space group P*nma* (Bjurstrom and Arnfelt 1929). The B atoms forming zigzag chains in FeB are in the interstices of Fe atoms in a distorted hexagonally close-packed arrangement, as shown in figure 1(*b*). A unit cell contains four equivalent Fe atoms and four equivalent B atoms in the positions of point group m (type B27, Fe with $x = 0.180$ and $z = 0.125$ and B with $x = 0.031$ and $z = 0.620$).

2.2. LAPW method and computation

The crystal potential is approximated in the warped muffin-tin (MT) form in this all-electron self-consistent calculation, i.e. a full potential without the shape approximation

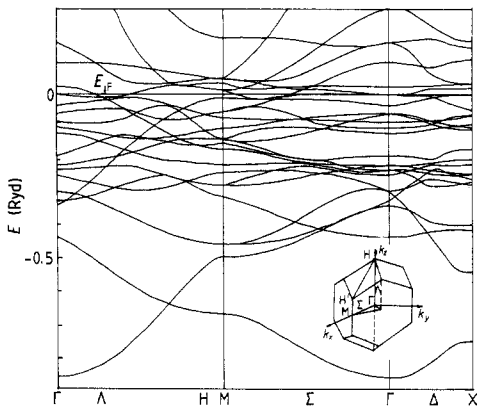

Figure 2. Energy bands of Fe_2B.

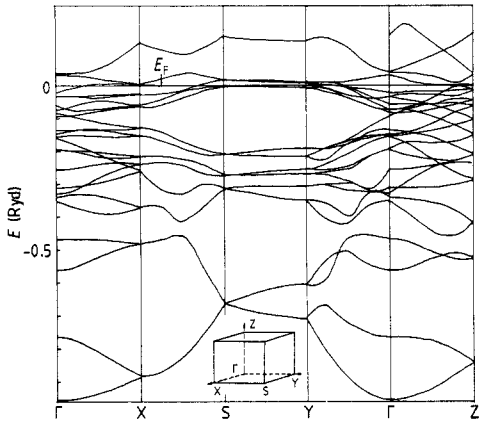

Figure 3. Energy bands of FeB.

in the interstitial region and a spherically symmetric potential inside the MT sphere are assumed. The core electrons are computed self-consistently for every iteration by a fully relativistic Dirac–Slater type of atomic structure program. The valence electrons are computed semi-relativistically, i.e. the Dirac equation is solved including mass–velocity and Darwin terms but without the spin–orbit coupling. Further details of the LAPW method are given in the paper by Koelling and Arbman (1975).

In both compounds, Fe 1s to 3p and *B* 1s are considered as core electrons and the radii of MT spheres of Fe and B atoms are 2.2 au and 1.4 au, respectively. The total volume of MT spheres is 54.34% of the unit cell in Fe_2B, and 50.55% in FeB. In Fe_2B, plane waves with an energy of 6.15 Ryd (about 270 LAPWs) and angular momentum components up to $l = 8$ are included in the basis function for all atoms. In FeB, plane waves up to an energy of 5.65 Ryd (about 290 LAPWs) and angular momentum components up to $l = 8$ are also included. Eight special $\boldsymbol{k}$-points in the irreducible Brillouin zone are used in both calculations to generate the charge density in self-consistent iterations. The self-consistency of calculation is assumed when the average difference between the input and output potential reaches 4 mRyd.

3. Energy bands and density of states

The calculated energy bands of Fe_2B and FeB are displayed in figures 2 and 3, respectively. The total density of states and local partial density of states, calculated by using the analytic tetrahedron interpolation (Rath and Freeman 1975), together with photo-electron spectroscopy (Joyner and Willis 1981) are shown in figures 4 and 5 for Fe_2B and FeB, respectively. In all figures of the local partial density of states, only the states below the Fermi energy are plotted.

It is clearly seen that the B 2s and 2p states in both compounds Fe_2B and FeB are located well below the Fermi energy. For Fe_2B the two lowest bands in figure 2 are contributions from the 2s states of two B atoms. That is, the interaction between two B atoms leads to the bonding and anti-bonding states and gives rise to two peaks in the plots of the density of B 2s states at about 0.68 Ryd (9.3 eV) and 0.60 Ryd (8.2 eV) below the Fermi energy (the peaks E and E′ in figure 4(*a*)). From about 0.60 to 0.20 Ryd below the Fermi energy, there are the degenerate B $2p_x$ and $2p_y$ states and B $2p_z$ state. At about 0.42 Ryd (5.7 eV) and 0.26 Ryd (3.6 eV) below the Fermi energy, there are two B 2p

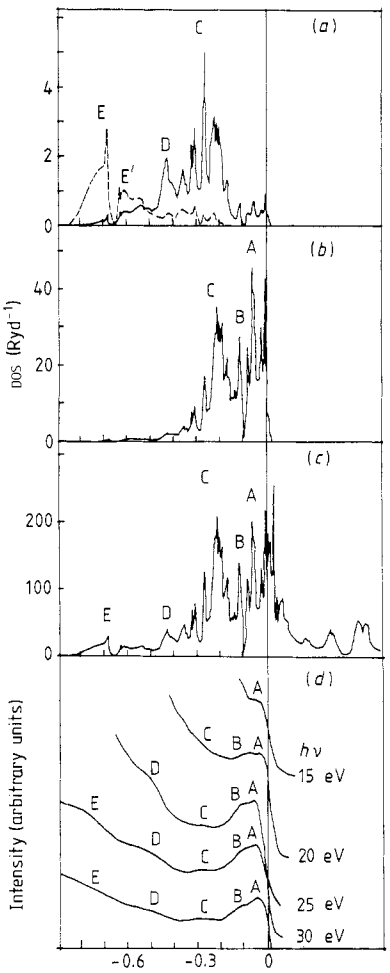

Figure 4. (*a*), (*b*) Local partial densities of states ((*a*) ----, B 2s, per B atom; ——, B 2p, per B atom; (*b*) Fe 3d, per Fe atom), (*c*) total density of states (per cell) and (*d*) photo-electron spectrum (after Joyner and Willis (1981)) for Fe_2B.

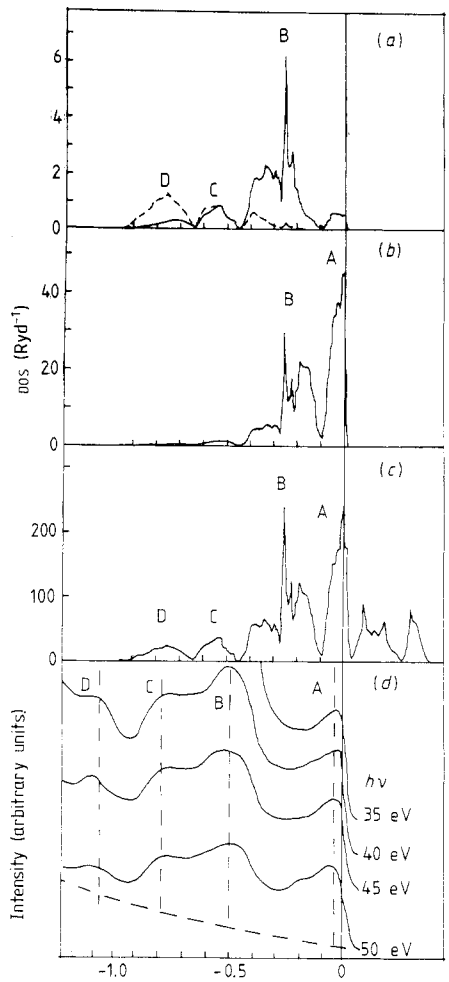

Figure 5. (*a*), (*b*) Local partial densities of states ((*a*) ----, B 2s, per B atom; ——, B 2p, per B atom; (*b*) Fe 3d, per Fe atom), (*c*) total density of states, per cell and (*d*) photo-electron spectrum (after Joyner and Willis (1981)) for FeB.

peaks (D and C in figure 4(*a*)). The latter B 2p peak coincides with an Fe 3d bonding peak. In this overlap region the interaction between Fe and B atoms makes the Fe 3d and B 2p states hybridise strongly. Another Fe 3d bonding peak (B in figure 4(*b*)) is at about 0.11 Ryd (1.5 eV) below the Fermi energy. Finally, near the Fermi energy there are two Fe 3d anti-bonding states. They form two peaks, one at 0.06 Ryd (0.8 eV) below the Fermi energy (peak A in figure 4(*b*)) and the other just at the Fermi energy (not labelled).

The distribution of the total density of states below the Fermi energy shown in figure 4(*c*) corresponds well to the five peaks obtained by photo-electron spectroscopy by Joyner and Willis (1981) and given in figure 4(*d*). The identification of the characteristics of these peaks based on the above analysis is given in table 1. It should be pointed out that, according to the analysis given by Joyner and Willis (1981), peak D in the photo-electron spectrum is the contribution from a hybridised B 2s–p state but, according to

Table 1. Identification of the peaks of the calculated density of states and the photo-electron spectroscopy data for Fe_2B.

Peak	Energy (eV)		
	Experimental	Theoretical	
A	≃0.8	0.8	Anti-bonding Fe 3d
B	≃1.4	1.5	Bonding Fe 3d
C	≃4	2.9, 3.6, 4.1	Bonding Fe 3d, B 2p
D	≃6	5.7	Bonding B 2p
E′	≃10.5	8.2	Anti-bonding B 2s
E		9.3	Bonding B 2s

the density of B 2s and 2p states shown in figure 4(*a*), the main overlap region of B 2s and 2p states is near the anti-bonding state of B 2s and its binding energy (E′ in figure 4(*a*)) is much larger than the energy of peak D in the photo-electron spectrum. Therefore, peak D should be the contribution from one of the B 2p states. According to the present calculation the peak from the B 2s–p hybridised state in Fe_2B is rather weak and is missing in the experimental curves. In table 1 it is also shown that the three calculated peaks which are close to each other correspond to peak C in the photo-electron spectrum. The peak of the Fe anti-bonding state located just at the Fermi energy is also missing in the photo-electron spectrum. Furthermore, we can analyse these peaks from their symmetry. The Fe atoms in Fe_2B are located at the position of the point group mm. Its five d states should split in energy. According to figure 4(*b*), there are the bonding states (peaks B and C) and anti-bonding states (peak A) below the Fermi energy. Another peak of the Fe anti-bonding state is located just at the Fermi energy. The higher peak above the Fermi energy in figure 4(*c*) should also be from one of the Fe 3d states. The B atoms in Fe_2B are at the position of the point group 42, and three B 2p states will split into a singlet and a doublet state (peaks C and D in figure 4(*a*)).

Peak C is caused by the overlap of Fe 3d and B 2p states. This means that the Fe 3d and B 2p electrons hybridise and form covalent bonds in this energy range. The extent of the overlap shows that the covalent bonds between the Fe and B are rather strong. These bonds between transition-metal atoms and metalloids, which occur in most interstitial compounds, play an important role in the properties, such as the cohesion of the compounds. The occurrence of peak E shows that covalent bonds exist between two B atoms formed by the 2s state. This is also seen in the contour plot of the constant electron density given below, but the contribution from these bonds to the cohesion is much less than from the bonds between Fe and B because both bonding and anti-bonding B–B bond states are occupied. In Fe_2B the B 2s–p state is so weak that it contributes little to cohesion. The general feature and the width of the curve of the density of Fe 3d states in Fe_2B are similar to those of metallic Fe, and this means that the metal bonds between Fe atoms are still prominent. So, in Fe_2B, many metal properties remain.

For FeB, the distribution of the density of states shown in figure 5 is roughly similar to that of Fe_2B. According to figure 5(*a*), the B 2s bonding peak is at about 0.75 Ryd (10.2 eV) below the Fermi energy, the overlap peak from the B 2p and Fe 3d states is at about 0.25 Ryd (3.4 eV) below the Fermi energy and the peaks of the Fe 3d anti-bonding states are still near the Fermi energy. However, many changes have occurred in the density of states for FeB with respect to that for Fe_2B. For example, the position of corresponding peaks in these two compounds shifts; the extent of the overlap of the B

Table 2. Identification of the peaks of the calculated density of states and the photo-electron spectroscopy data for FeB.

Peak	Energy (eV)		
	Experimental	Theoretical	
A	0.06	0.05	Anti-bonding Fe 3d
B	6.6	2.5, 3.4, 4.4	Bonding Fe 3d, B 2p
C	10.5	7.2	Bonding B 2s, 2p
D	14.0	10.2	Bonding B 2s

2p and Fe 3d states is even weaker than that in Fe_2B. It should be emphasised that the most important change is that the overlap of B 2s and 2p states is predominant in FeB. In figure 5(*a*), we may clearly see the overlap of the two states and the peak (peak C in figure 5(*a*)) generated by them at about 0.53 Ryd (7.2 eV) below the Fermi energy. Therefore, in FeB, the B 2s and 2p states strongly hybridise into 2s–p and form covalent bonds between the B atoms. The identification and comparison with the photo-electron spectroscopy data are given in table 2. The changes in the density of states for FeB, compared with that for Fe_2B, reveal that on increase in the B content the electron transfers from the covalent Fe–B bonds to the covalent B–B bonds. In FeB the covalent bonds between B atoms dominate the cohesion, as discussed by Joyner and Willis (1981).

In both compounds Fe_2B and FeB, the states at the Fermi energy mainly come from the d states of the Fe atom, as shown in figures 4 and 5. The density $N(E_F)$ of states at the Fermi energy per Fe atom is about 40 Ryd^{-1} (about 3 eV^{-1}). On the assumption that the Stoner parameter I is 0.92, the same as for metallic iron (Gunnarson 1976), then the criterion $IN(E_F)$ is certainly larger than unity, which means that ferromagnetism is expected for these two compounds Fe_2B and FeB, according to the Stoner model.

A difference exists between the position of the peaks for the calculated density of states and that measured by photo-electron spectroscopy in both compounds Fe_2B and FeB. The calculated binding energy is usually less than the measured value. This difference is quite prominent for peaks B, C and D in FeB. Neglect of the state- and energy-dependent core–hole relaxation in the present single-particle approximation is one of the reasons. Indeed from tables 1 and 2 it is seen that the effect is small in the vicinity of the Fermi energy as discussed by Davis (1986). For low-lying B 2s and B 2p states the difference in Fe_2B is about 1 eV and in FeB is about 3 eV. The same difference has also been noted by Joyner *et al* (1981).

4. Charge density and bonding

On the basis of previous analyses, in Fe_2B, B 2p and Fe 3d states hybridise and form strong covalent bonds. According to the crystal structure (figure 1(*a*)), these bonds connect B to eight neighbouring Fe atoms. To demonstrate these bonds, the valence charge density in a (120) plane through B and Fe atoms is shown by a contour plot of the constant electron density in figure 6. The shape of the contour showing the electron concentration along the line connecting Fe and B reveals the covalent character. 16 such bonds are distributed uniformly over the whole space of a unit cell. So it is anticipated that a large increase in the cohesion would be affected for Fe_2B with respect to the pure metal Fe. From figure 6, we can also inspect the bonding between the two B atoms,

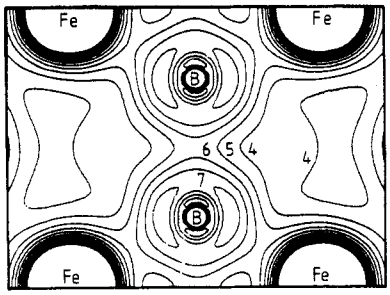

Figure 6. Contour plot of constant valence electron density (in units of 0.01 au^{-3}) of Fe_2B on the (120) plane through B and Fe atoms. The B–B distance is 4.03 au and the Fe–B distance is 4.12 au.

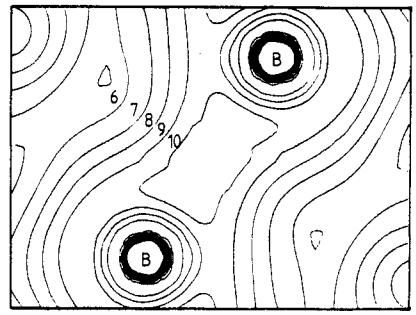

Figure 7. Contour plot of constant valence electron density (in units of 0.01 au^{-3}) of FeB on a vertical plane containing two adjacent B atoms. The B–B distance is 3.36 au.

Table 3. Total and *l*-decomposed number of valence electrons in MT spheres for Fe_2B and FeB.

		Number of valence electrons			
Compound	Site	s	p	d	Total
Fe_2B	Fe atom	0.3205	0.3907	6.0726	6.8153
Fe_2B	B atom	0.3654	0.6329	0.0161	1.0157
Fe_2B	Interstice				8.8277
FeB	Fe atom	0.2973	0.4027	6.1631	6.8974
FeB	B atom	0.3667	0.6785	0.0171	1.0637
FeB	Interstice				12.2817

which shows a covalent character and corresponds to peak E in the density of states or photo-electron spectrum, as discussed above.

According to the crystal structure of FeB, B atoms forming zigzag chains are in the interstices surrounded by Fe atoms, and the distance between two B atoms is 3.36 au (in Fe_2B it is 4.03 au). The interaction between B atoms is rather strong. According to the analysis in § 3, the strong interaction between the B atoms causes a 2s–p hybridisation and leads to strong covalent bonds. The valence electron density of a vertical plane containing two B atoms is given in figure 7. It is clearly shown that there exists an even stronger bond between the two B atoms. The electron density at the centre of B–B bonds in FeB is 0.1 electron au^{-3}, which is almost twice as much as that in Fe_2B. It is this strong covalent bond which makes the B atoms form linear zigzag chains in FeB. The B chains may be considered as a pseudo-one-dimensional system; so it is anticipated that the corresponding behaviour and properties should occur in FeB.

5. Electron transfer

In the LAPW method, the unit cell is divided into two regions, i.e. the MT spheres and the interstitial region. Here the electron transfer is given in terms of the change in the number of electrons in the corresponding spherical region. Table 3 shows the number

Table 4. Core levels of Fe and B atoms in Fe_2B and FeB with respect to the Fermi energy.

	Core level (Ryd)						
	Fe 2s	Fe $2p_{1/2}$	Fe $2p_{3/2}$	Fe 3s	Fe $3p_{1/2}$	Fe $3p_{3/2}$	B 1s
				Theoretical data			
Fe_2B	−59.588	−51.385	−50.471	−6.348	−3.951	−3.837	−12.432
FeB	−59.584	−51.384	−50.469	−6.338	−3.960	−3.846	−12.352
				Experimental data (Joyner and Willis 1981)			
Fe	−62.14	−52.94	−51.98	−6.71	−3.90		
Fe_2B	−62.11	−52.96	−51.99	−6.74	−3.90		−13.83
FeB	−62.14	−52.96	−52.00	−6.74	−3.92		−13.82
B							−13.82

of valence electrons decomposed according to the angular momentum in the Fe and B MT spheres in the two compounds. The total number of electrons in the B MT sphere increases by about 0.05 in FeB with respect to Fe_2B. At the same time the total number of electrons in the Fe MT sphere also increases by about 0.08 electron. Roughly speaking, no electron transfer happens between Fe and B atoms on comparing the two compounds with each other. Furthermore, table 4 shows the core levels of Fe and B atoms of the two compounds. The calculated results show that the energy levels of all Fe core states do not change (by less than 0.1 eV), which coincides with the photo-electron measurements (Joyner and Willis 1981), but the energy level of the B 1s core state changes about 1.1 eV in FeB with respect to Fe_2B, which is different from the photo-electron measurements.

There is about one electron in the B MT sphere in both Fe_2B and FeB, in agreement with the results given by Brown and Cox (1971) and Perkins and Brown (1974), but according to the present paper this electron is contributed from the occupied local 2s and 2p states.

6. Isomer shift

Electrostatic interaction between the nucleus and its environment gives rise to the isomer shift, which can be measured by Mössbauer spectroscopy:

$$\Delta v = \alpha(\Delta\rho(0))$$

where $\alpha = -0.26\ \text{mm s}^{-1}\ \text{au}^{-3}$ (Zhang *et al* 1987) and $\Delta\rho(0)$ is the difference between the electron density at the Fe nucleus for the systems under consideration (Fe_2B and FeB) and that for the reference material (metallic Fe).

The electronic density at the Fe nucleus in Fe, Fe_2B and FeB, the difference between borides and Fe, and the calculated isomer shift are given in table 5, together with the experimental results (Cooper *et al* 1964). The positive isomer shift is due to the decrease in the Fe 4s electron caused by the interaction between Fe and B atoms in the two compounds and the increase in the 3d electron in the Fe MT sphere, which leads to a stronger screening of the Fe 3s electron and thus a decrease in the density of the Fe 3s electron at the Fe nucleus.

7. Conclusion

This paper self-consistently calculates the electronic structures of two interstitial compounds Fe_2B and FeB from first principles. The results show that B 2s and 2p states are

Table 5. The density $\rho(0)$ of electrons at the Fe nucleus and increment $\Delta\rho(0)$ with respect to the metal Fe and isomer shift.

	FeB	Fe_2B	Fe
$\rho(0)$, 1s	13300.961	13300.876	13300.855
$\rho(0)$, 2s	1247.014	1246.816	1246.767
$\rho(0)$, 2p	6.821	6.819	6.819
$\rho(0)$, 3s	181.825	182.026	182.666
$\rho(0)$, 3p	0.951	0.953	0.958
$\rho(0)$, 4s	5.963	6.419	6.722
$\rho(0)$, total	14743.535	14743.909	14744.787
$\Delta\rho(0)$	−1.252	−0.878	
Theoretical isomer shift (mm s^{-1})	0.228	0.326	
Experimental isomer shift (mm s^{-1}) (Cooper *et al* 1964)	0.11	0.28	

below the Fermi energy in the two compounds. The calculated density of states is in agreement with the photo-electron spectrum given by Joyner and Willis (1981). In Fe_2B there exists a rather strong overlap peak of Fe 3d and B 2p states, which leads to a strong covalent bond between the Fe and B atoms and dominates the cohesion of Fe_2B. Both the bonding and the anti-bonding states of B 2s are occupied; so they contribute less to the cohesion. The calculated B 2s–p peak is very weak and is missing from the photo-electron spectrum. The density of Fe 3d states for Fe_2B is similar to that for metallic Fe, and the metallic bonds between Fe atoms is still prominent. The curve of the density of states for FeB is roughly similar to that for Fe_2B. The most important change is that the B 2s and 2p states in FeB hybridise into 2s–p states and form rather strong covalent bonds, which cause one-dimensional zigzag chains of B atoms in FeB. The combination of the covalent Fe–B bonds and metallic Fe–Fe bonds in Fe_2B and the combination of the covalent B–B bonds and metallic Fe–Fe bonds in FeB are characteristic properties of interstitial compounds. No electron transfer either from B to Fe or from Fe to B occurs in these two compounds.

Acknowledgments

This work is supported by the National Science Foundation of China through Grant 84W17. One of the authors (Li) wishes to express his thanks to Mr Ruqian Wu for helpful discussions.

References

Andersen O K 1975 *Phys. Rev.* B **12** 3060
Bjurstrom T and Arnfelt H 1929 *Z. Phys. Chem.* B **4** 469
Brown P J and Cox J L 1971 *Phil. Mag.* **23** 705
Cooper J D, Gibbs T C, Greenwood N N and Parish R V 1964 *Trans. Faraday Soc.* **10** 2097
Davis L C 1986 *J. Appl. Phys.* **59** R25
Gunnarson O 1976 *J. Phys. F: Met. Phys.* **6** 587
Hedin L and Lundquist B J 1971 *J. Phys. C: Solid State Phys.* **4** 2064
Johnson O, Joyner D J and Hercules D M 1980 *J. Phys. Chem.* **84** 542

Joyner D J, Johnson O and Hercules D M 1980a *J. Am. Chem. Soc.* **102** 1910
—— 1980b *J. Phys. F: Met. Phys.* **10** 16
Joyner D J, Johnson O, Hercules D M, Bullett D W and Weaver J H 1981 *Phys. Rev.* **24** 3122
Joyner D J and Willis R F 1981 *Phil. Mag.* **43** 815
Koelling D D and Arbman G O 1975 *J. Phys. F: Met. Phys.* **5** 2041
Perkins R S and Brown P J 1974 *J. Phys. F: Met. Phys.* **4** 906
Rath J and Freeman A J 1975 *Phys. Rev.* B **11** 2109
Wever F and Muller A 1930 *Mitt. K. Wilhelm-Inst. Eisenforsch., Dusseldorf* **11** 193
Zhang Qi-ming, Zhang Yu-lin and Wang Ding-sheng 1987 *Commun. Theor. Phys.* **8** 139